

# Interactions Between Urban Heat Island and Localized Microclimate Precipitation in Albuquerque, New Mexico

*H. Fox-Gardner*<sup>a</sup>

*N. Smith*<sup>a</sup>

*L. E. Silbert*<sup>a</sup>

*M. W. Cole*<sup>a\*</sup>

<sup>a)</sup> Central New Mexico Community College, Albuquerque, NM, USA

## ABSTRACT

The Urban Heat Island Effect (UHIE) is known to significantly impact broad city-scale regions by elevating air and surface temperatures in urban environments relative to adjacent rural areas, commonly quantified as the urban–rural temperature differential. While regional-scale studies have demonstrated a link between UHIE-induced thermal anomalies and enhanced convective activity influencing precipitation dynamics, experimental research exploring UHIE impacts at microclimatic scales remains limited. To investigate the relationship between localized thermal anomalies and precipitation, we conducted a microclimate study focused on a well-defined urban hotspot characterized by impervious surfaces and sparse vegetation in Albuquerque, New Mexico. Pedestrian-level air and surface material temperature data were collected along a 2-mile closed-loop transect. A stationary weather station located near the transect location provided the precipitation data, while a stationary temperature/relative humidity data logger placed in a non-urban zone served as a reference for rural baseline temperatures to calculate UHIE intensity. We find a robust correlation of 60.9% and 66.4% between air and surface material temperatures such that extensive asphalt and concrete coverage contributed to pronounced heat retention and marked temperature “spikes” preceding precipitation events compared to rural baselines. These results underscore that reciprocal interactions among temperature, urban materials, and precipitation at even the microclimate-local scales are genuine and consequential. Advancing our understanding of these dynamics is essential for informed urban planning and the development of climate resilience strategies amid increasing urbanization and extreme weather patterns.

**KEYWORDS:** Urban Heat Island, Microclimatics, Thermal anomalies and precipitation

## 1 INTRODUCTION

The Urban Heat Island Effect (UHIE) is indicative of high temperatures in urban areas when compared to rural surrounding areas, due to heat absorbing materials used in urban development. This effect was first observed by Luke Howard (1833) and later studied in the 1950s (Sundborg, 1950), when it was documented that the dense nature of cities with large obstructing buildings were creating their own microclimates. While numerous studies have examined UHIE Intensity (UHIEI) and its influence on precipitation patterns, most have focused on broad regional impacts.

These effects are known to bifurcate storms around large urban centers due to the thermodynamic entropic property effects of man-made materials that make up urban centers (NASA Earth Observatory, 2006) as well as urban aerosols and wind-blocking geometry of man-made structures. This large regional effect often results in decreased precipitation within urban centers and increased precipitation downwind of urban centers, increasing the risk of flood-related jeopardy in those regions (Mingze Ding, 2025).

While these regional UHIE findings are valuable, they miss the influence of urban microclimates—revealing a key gap in spatial resolution. Most of the studies into this phenomenon used vehicles to collect data that might influence their data. This study addresses that gap by analyzing surface composition, temperature, and precipitation at the neighborhood scale by collecting data on foot, underscoring the need for fine-scale data to capture urban climatic complexity.

In 1921, Robert Horton was the first to discover that cities create their own weather patterns, while observing Albany, NY and Providence, RI. He observed that there were thunderstorms that formed over cities, and dissipated not far outside of city limits. He believed that cities (urban centers) might create favorable conditions for thunderstorms to form, though at the time he was unsure what those conditions were (Horton, April 1921).

UHIE-induced precipitation was confirmed in a study that was conducted in 1971 in St. Louis, MO and St. Louis, IL called METROMEX (METROPolitan Meteorological EXperiment) (Changnon J. S., 1971). They collected their data using meteorological vehicles (surface temperatures, wind, and humidity) a radiosonde unit west of St. Louis, and four pibal stations around the perimeter of the urban center. They collected rainfall and air samples to identify if urban pollution contributed to the precipitation events. Their findings were that urban centers, due to the urban heat island effect and pollutants endemic to urban centers, contributed to an increase rate of convective rainfall downwind of the city.

UHI-induced precipitation events are defined by the Brown and Arnold weak synoptic environment methodology using the following three criteria: (1) no synoptic surface forcing within 500 km (this includes pressure systems, fronts, and outflow boundaries), (2) wind speeds below 15 knots (7.71667 m/s) at 500 hPa, (3) wind speeds below 10 knots (5.14444 m/s) (Brown, 1998).

A more recent study in Atlanta, GA, during warm seasons, identified 37 instances of UHI-induced precipitation between 1996- 2000, using radar reflectivity, over the course of 20 days (Dixon, 2003). During their study they also found a correlation with low-level moisture content and UHI intensities. We had similar findings, in that we had high initial relative humidity readings on ground level, preceding our UHI-induced precipitation, relative humidity decreased dramatically from 55- 60% to 20- 25% immediately preceding each event. Their study showed a correlation with higher dewpoints and UHI-induced precipitation, but our study showed that while peaks in dewpoint did occur previous to UHI-induced precipitation, it preceded naturally occurring storm front precipitation as well. This indicates that peaks in dewpoint are not unique to UHI-induced precipitation.

## **2 METHODOLOGY**

This study was designed with the purpose of analyzing the Urban Heat Island – induced precipitation events in a heavily commercialized area in Albuquerque. The study area is shown in Figure 1. The transect location was selected due to its high probability of demonstrating an archetypical

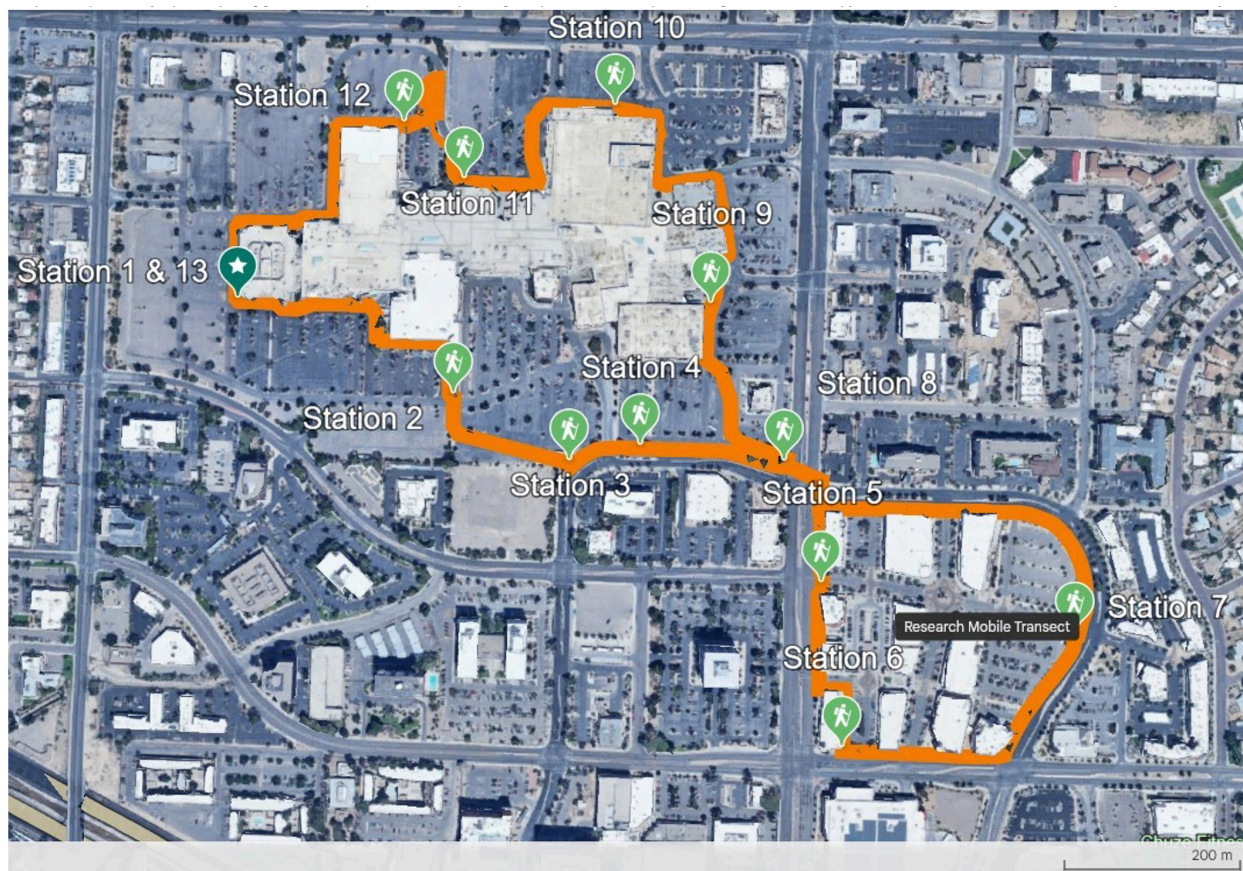


Figure 1. Aerial image showing the Coronado/Uptown 2-mile closed loop transect. The orange line represents the transect walking path (approximately 3,324 m or 2.05 mi) and the green pins represent the 13 data collection sites for the ground truth air temperatures (Google Earth, 2023).

The transect area is primarily composed of public commercial spaces around the perimeter of the Coronado and the Uptown Shopping Centers. The buildings contained within, and immediately surrounding, the transect area are primarily two to three story buildings, with two six-story hotels, and one ten-story office building. These public spaces are primarily composed of asphalt parking areas, and concrete sidewalks. Small green spaces within the study area consist mostly of smaller trees, with a small number of larger trees, and small foliage. Concrete and asphalt surfaces are comprised of an estimated 95% of the overall surface areas surrounding the buildings. For the scope of our study, we designed a two-mile closed loop transect with thirteen stations (Figure 1). Each of the stations is five minutes walking distance from one another. The transect was traversed on foot twice a week (Sunday and Wednesday), three times a day (8:00– 9:00 am, 2:00– 3:00 pm, and 7:00– 8:00 pm) during our 8-week data collection period. At each station environmental data was collected using four sensor devices, specifically, an AirBeam 3 logger [air temperature (°F); resolution: 0.1°C], a Kestrel 3000 hand-held spot sensor (air temperature (°F) and wind speed (mph); resolution: 0.1 °C, 0.1 mph), a PocketLab Air logger [barometric pressure (mbar); resolution: 1.3 Pa], and a Thermoworks IRK-2 IR [materials temperature (°F); resolution: 0.1° from -83.2 to 999.9°]. Data collection took place from May 27, 2024, through July 24, 2024. To establish a rural temperature baseline, a HOBO MX2300 weather station [air temperature (°F), relative humidity (%), and dewpoint (°F); resolution: 0.02 °C (0.036 °F)] was deployed in Tijeras, NM, approximately 7.19 mi (11.57 km) east of Albuquerque (Figure 2), near a researcher’s residence in

Cibola National Forest. Tijeras, NM was chosen due to a lower percentage of manmade material ground cover (70% natural materials and vegetation), in contrast to the transect location in Albuquerque which has a higher percentage of manmade material ground cover (13% natural materials and vegetation) (The Nature Conservancy New Mexico, 2025). Tijeras, NM also has a lower population density with only 483 people residing in the village (DATA USA, 2023), as compared to Albuquerque, NM with a population of 564,559 (Census.gov, 2020). This location was selected for its relative distance from urban infrastructure, providing a reliable reference point for ambient rural conditions, and to address vulnerabilities related to the security of our sensor devices (2 HOBO stations that had been deployed in Albuquerque in rural areas, were misappropriated by persons unknown). The San Pedro and Uptown (LoboNet) (University of New Mexico, 2024) stationary weather station located near our transect-site, provided additional data on both wind speed and precipitation rate.

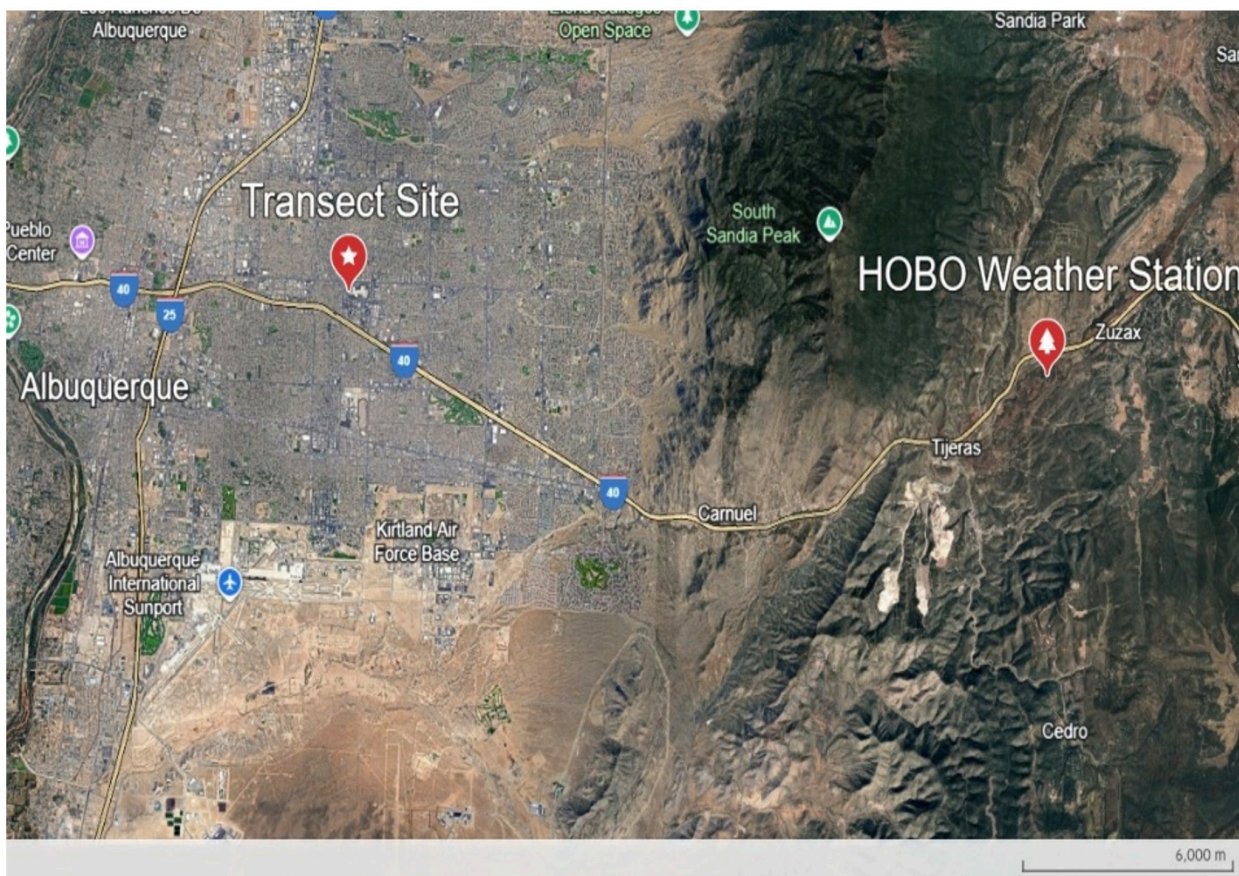


Figure 2. Map of distance between urban transect site and rural HOBOWeather Station (Google Earth, 2022–2025).

Air temperature measurements were acquired using an AirBeam 3 handheld logger sensor equipped with a solar radiation shield, recording data at one-second intervals. Due to the sensor's solar casing, the raw temperature readings exhibited a consistent positive bias relative to ambient conditions, necessitating post-collection thermal calibration. To establish accurate ground-truth values, a Kestrel-3000 manual handheld sensor, with open casing was used to collect at each of the 13 stations, to compare and curve fit data from the AirBeam 3. Most of the sensors used

were calibrated at the manufacturer, however the air temperature data which was collected via an AirBeam solar-radiation-shielded hand-held air-sensor required calibration. To accomplish this a Kestrel-3000 sensor (ground-truth/TAIR) was used for temperature calibration. The corrected temperatures were obtained utilizing Kestrel data in combination with a mathematical model employing a second-order polynomial curve-fitting protocol (Will-Cole, 2025). The 13 stations were used as the points of calibration within the transect for the AirBeam.

### 3 RESULTS

We hypothesize that our transect site exhibits a pronounced Urban Heat Island (UHI) effect, indicative of a distinct microclimate within the broader urban landscape. Evidence supporting our hypothesis that there was modification to localized precipitation was found on June 19, June 24, July 18, July 21, and July 24 (Figure 3). On these dates UHIE-induced precipitation incidents were recorded by our sensors. The events were initiated by high surface temperature readings and high relative humidity, and we witnessed cloud formation directly over the region of Albuquerque that contained our transect study area.

These five days were identified with spikes in  $\Delta T$  followed by precipitation events. Of the five days, one day (6/19/2024) was negated because it failed all three of the criteria from the Brown and Arnold methodology for determining UHI-induced precipitation (Brown, 1998).

Our study indicated that the greatest indicators of UHI-induced precipitation were high surface temperatures, a spike in convective available potential energy from surface (CAPE), a localized spike in  $\Delta T$ , a decline in relative humidity of 25- 30%, which strongly paralleled a decline in barometric pressure, followed by precipitation. By the afternoon, there was a dramatic drop in relative humidity, barometric pressure, and surface temperatures. However, the  $\Delta T$  (the difference between

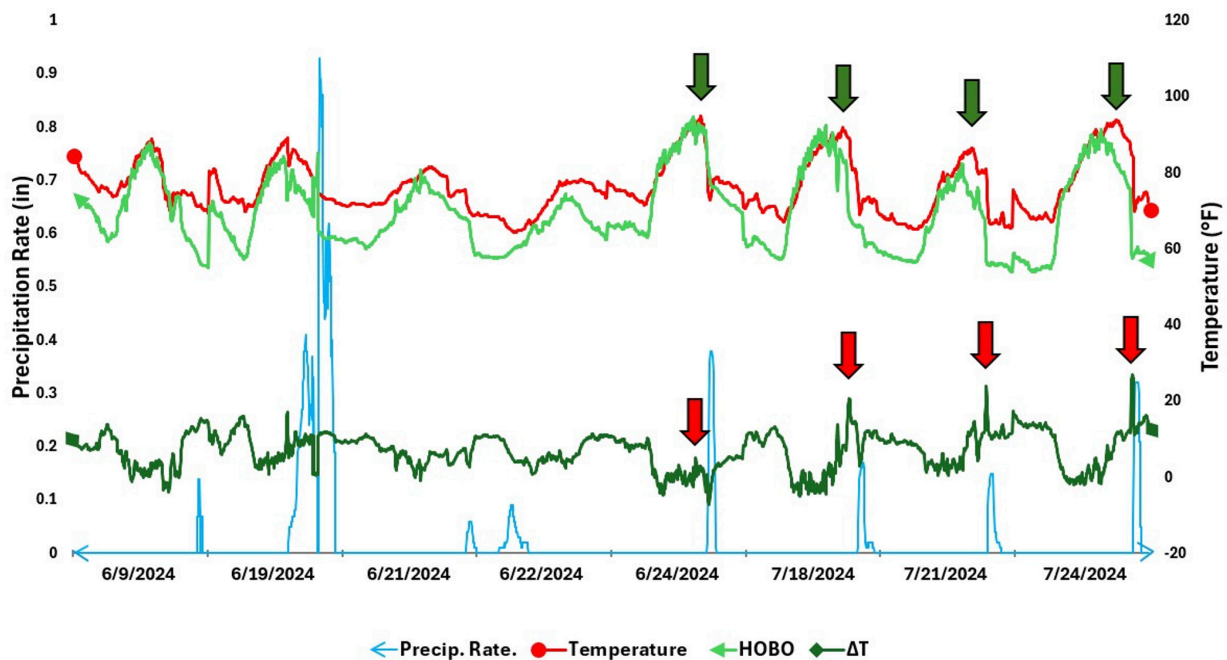


Figure 3. All days with precipitation during data collection dates. Transect location temperature (red) – rural temperature (light green) =  $\Delta T$  temperature (dark green) vs. precipitation (light blue). Arrows indicate  $\Delta T$  temperature spikes preceding UHIE modified precipitation events.

**TABLE 1. Applying Brown and Arnold weak synoptic environment methodology to identify days. (Beccario, 2025)**

Time Stamp	Wind Speed 500 hPa (m/s)	Threshold 500 hPa (m/s)	Wind Speed 850 hPa (m/s)	Threshold 850 hPa (m/s)
6/19/2024 14:31	15.2	14.4	8.4	7.7
6/24/2024 15:36	5.4	14.4	3.7	7.7
7/18/2024 19:12	2.7	14.4	7.9	7.7
7/21/2024 19:19	9.4	14.4	6.5	7.7
7/24/2024 21:01	7	14.4	3.7	7.7

transect and rural air temperatures) remained within the normal 10- 20 °F range expected for a city with a UHI. The rural location had started to decline in temperature, but the transect site temperatures continued to climb. This only occurred on 6/19, 6/24, 7/18, 7/21, and 7/24, immediately preceding a precipitation event. Other days 6/9, 6/21, and 6/22, which also had precipitation, and days that did not have precipitation, did not have a spike in  $\Delta T$ . By the time of the evening transects wind gusts had elevated to between 10- 20 mph, and the air temperature differential between the transect site and the rural HOBO station ( $\Delta T$ ) spiked to between 5- 27 °F. These spikes in air temperature preceded precipitation in each event.

These events differed from an unmodified (natural storm-fronts, verified from weather maps of pressure fronts) (National Weather Service, 2025) rainfall event, that also occurred during our data collection dates, due to the drastic spike in  $\Delta T$  (Figure 3) and the steep drop at ground level, in relative humidity preceding the rainfall event. This temperature difference occurred over periods as short as 15- 20 min, and up to 120 min. These differences were concurrent with the wind gust front appearance, and a drop in barometric pressure, and were immediately followed by precipitation.

The relative humidity was also analyzed using the Nullschool Earth modeling tool (Beccario, 2025) on those dates that experienced rain during the data collection period. A pattern was observed on the days June 19 and 24, July 18, 21, and 24 showing a decrease in relative humidity, (from 50- 60% during the morning transect) at ground level (to 22- 38% just previous to precipitation), and a low condensation level saturation of 61- 79% relative humidity at the condensation level of 500 hPa at an approximate equivalent of 5000 m above sea level (Beccario, 2025), before a precipitation event (Figure 4).

Although June 19 shared similarities with the other four days, after applying the Brown and Arnold methodology for determining UHI-induced precipitation, it was determined that there was a high/low pressure front directly overhead during the precipitation event, and wind speeds at 500 hPa (15.2 m/s) and 850-hPa (8.4 m/s) both exceeded boundary limits. June 19 was likely a monsoonal storm front and is negated, due to the methodology for determining UHI-induced precipitation, however, the similarities to the other four days, may be relevant for future discussions, as to interactions between UHI-induced precipitation and monsoonal inputs.

Anecdotally, more ambulances were observed near our transect on days that these  $\Delta T$  spikes occurred, but further studies will need to be done, to understand if there is a relationship between the  $\Delta T$  spikes and human health.

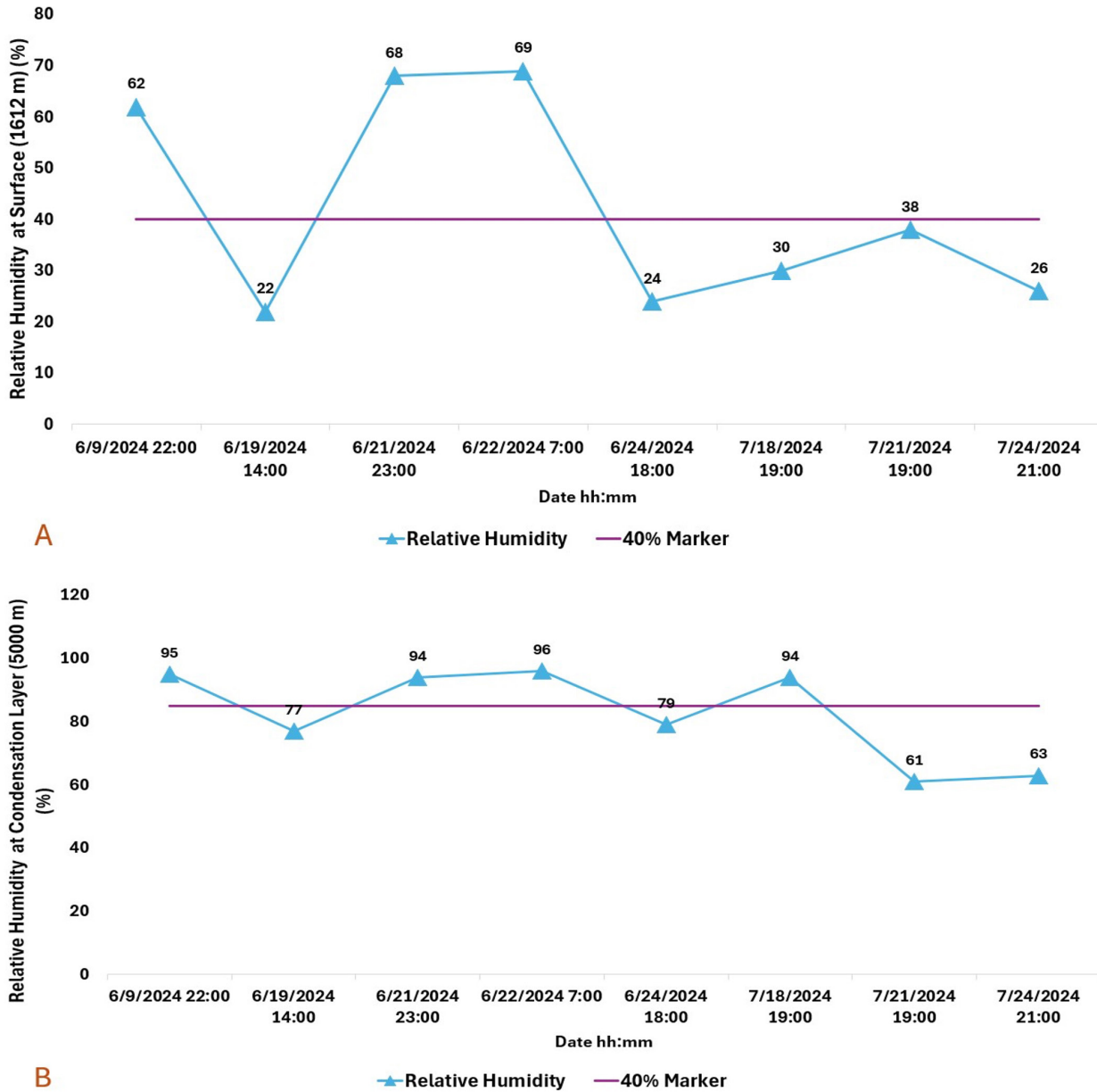


Figure 4. Relative humidity at the surface level (1612 m) and at the condensation level (5000 m). (Beccario, 2025)

#### 4 DISCUSSION

This study was designed to answer two primary research questions. Is there a UHIE occurring in Albuquerque, NM? What effect does it have on the localized precipitation?

We quantified the UHIE by calculating the temperature difference between the onsite transects readings and the rural HOBO station readings, referred to as  $\Delta T$ . Air temperature  $\Delta T$  was elevated between 10- 20 degrees Fahrenheit above rural values, supporting our hypothesis that there is a significant UHIE at the transect location

Ambient air temperatures were compared to cement and asphalt surface temperatures at each of

transect locations (Figure 5). Ambient air temperatures (Kestrel) were consistently similar at all 13 stations along the transect. However, there was a noticeable difference with the cement and asphalt surface temperatures (IRK) at one of the stations. Station 4 was a bus stop adjacent to the Coronado Mall, that had larger trees shading it, and it showed a significant drop in both cement and asphalt surface temperatures as a result. Since station 4 is an anomaly in the data, the remainder of the data analysis will negate it.

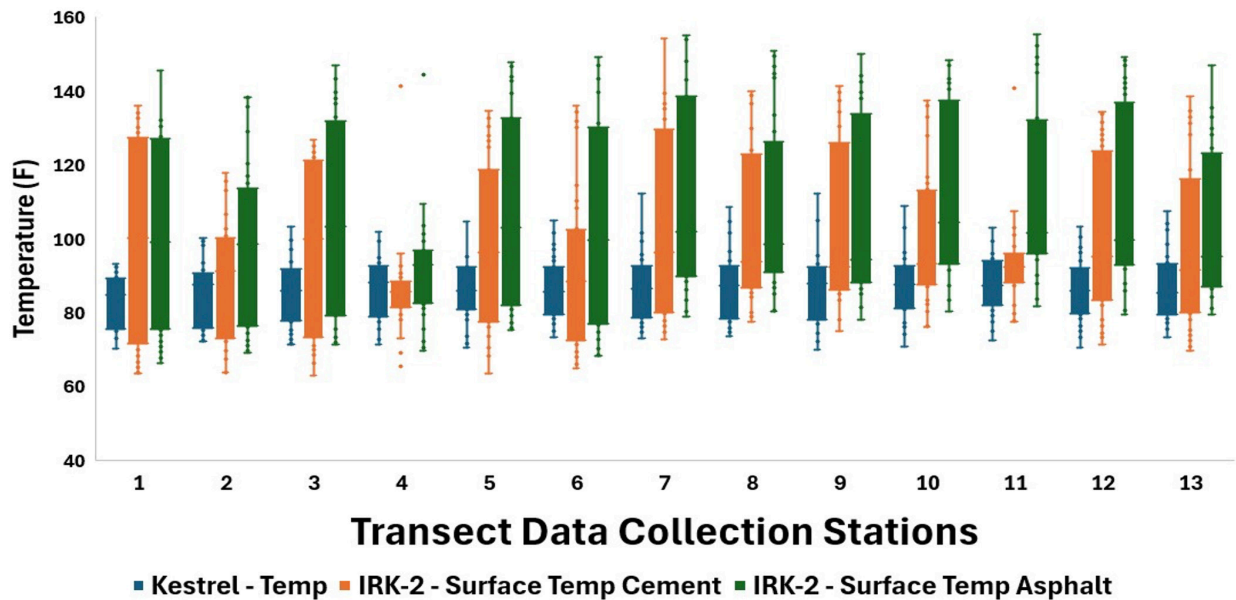


Figure 5. Comparison of ambient air temperature and the surface temperatures of cement and asphalt at the mobile transect data collection stations.

The spikes in  $\Delta T$  were the direct result of the high asphalt and concrete surface temperatures that ranged from 140- 160 degrees. These surface temperatures were the direct result of solar radiation that was absorbed by the asphalt and concrete and was re-emitted as infrared radiation. By the conservation of energy principle, these energy values are equivalent.

$$E_{\text{solar radiation absorbed by surfaces}} = E_{\text{infrared radiation from surfaces}}$$

Since localized temperature differences, not the global average, were the focus of this study, we calculated the infrared radiation emitted by asphalt and concrete. We used thermodynamics principles to analyze exclusively re-emitted infrared radiation from the manmade surfaces at that transect location so we could compare them with relative humidity readings taken simultaneously on site (Figure 6). We did this using our readings recorded during the transects and the Stefan-Boltzmann law ( $F = \sigma T^4$ ), for the total surface area of the transects area (Figure 6). The total emissive power or radiant exitance (F) was calculated and input into the graph (Figure 6), by multiplying the temperatures collected during the mobile transect, in Kelvin to the fourth power, multiplied by the Stefan-Boltzmann constant ( $5.67 \times 10^{-8} \text{ W}/(\text{m}^2 \cdot \text{K}^4)$ ). During our data collection, we had access to public areas surrounding the buildings contained in the transect area. Building roofs were off-limits for the purpose of this study. Therefore, the total surface area was calculated by determining the total area ( $399,001 \text{ m}^2$ ) using Google Maps, then subtracting the area of all buildings present in the transect area ( $103,676 \text{ m}^2$ ). This gives a total surface area of  $295,325 \text{ m}^2$ . Since the amount

of cement is negligible in relation to the amount of asphalt, we negated the cement for this calculation. The max value of energy emitted from the total area of the site on 7/7/2024 was over 351.7 Kw. It is important to note that asphalt does not reradiate heat at the same rate that it is absorbed. To calculate the absorption (how much energy is needed to heat the asphalt) and the heat reradiation (how much energy is reradiated from the asphalt), we used the heat capacity equation  $Q = mc\Delta T$  formula. Mass (m) was calculated from total area and thickness of the asphalt. Specific heat (c) was calculated from the emissivity index for asphalt of 0.92. The  $\Delta T$  was calculated for heat absorption, by subtracting the morning surface temperatures from the afternoon surface temperatures. The  $\Delta T$  for infrared radiation was calculated by subtracting afternoon surface temperatures from evening surface temperatures. These calculations were done for each of the 13 data collection stations. Then an average was calculated for both the heat capacity and heat transfer capacity, and the heat transfer capacity was divided by the heat capacity. It was determined that while

$E_{\text{solar radiation absorbed by surfaces}} = E_{\text{infrared radiation from surfaces}}$  it takes 62.8% longer for  $E_{\text{infrared}}$  to equal  $E_{\text{solar}}$ . This is of particular importance for the UHI-induced precipitation that occurred on 7/24/2024 at 9:01 p.m., after the sun set. Absorption of solar radiation is significantly faster than radiant long-wave energy release from asphalt surface areas.

These measurements (Figure 6) were overlaid with relative humidity data to demonstrate that the vehicle for the heat transference to the air temperature was relative humidity. On days where the relative humidity was high, the surface temperatures are significantly lower. Water vapor, which is a natural and strongest greenhouse gas, absorbs the infrared heat emitted by the asphalt and concrete surfaces (Easterbrook, 2016), which through natural thermodynamic processes transfers heat energy from surfaces and captures that energy through use of the hydrogen bond bridge (Jahnke, 2010). The presence of water vapor in a given parcel of air increases ambient air temperatures, which lowers parcel density and increases buoyancy relative to the surrounding air. Our data showed a high correlation between surface temperatures and ambient air temperatures of 0.609 and 0.6635 when compared on a scatterplot of air temperatures and surface temperatures (Figure 7). The heated ambient air creates an upward force that carries the heated water vapor higher into the

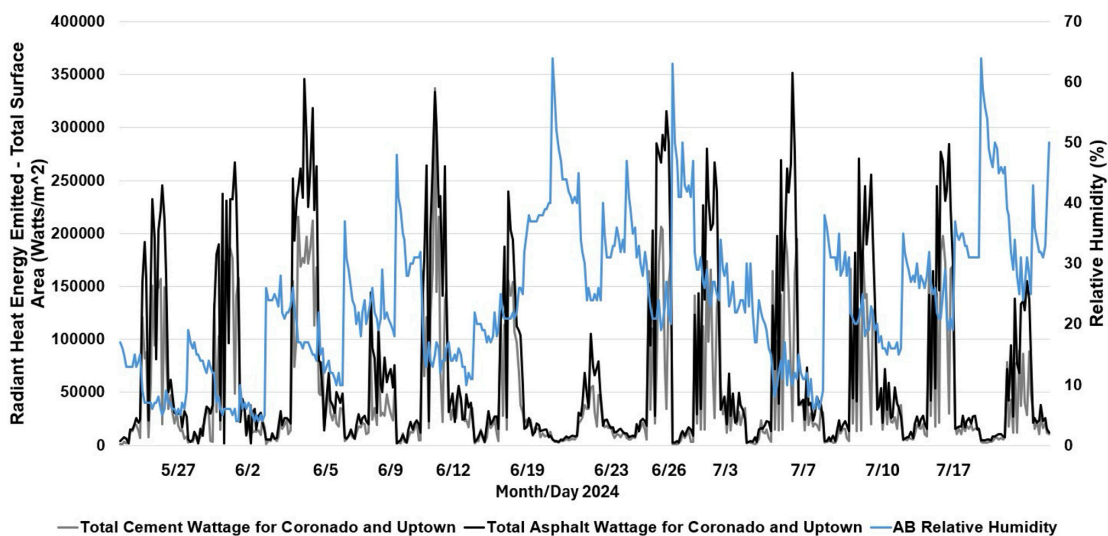


Figure 6. Total energy absorbed and reemitted by the Coronado Mall and Uptown Shopping Center by total area vs the relative humidity.

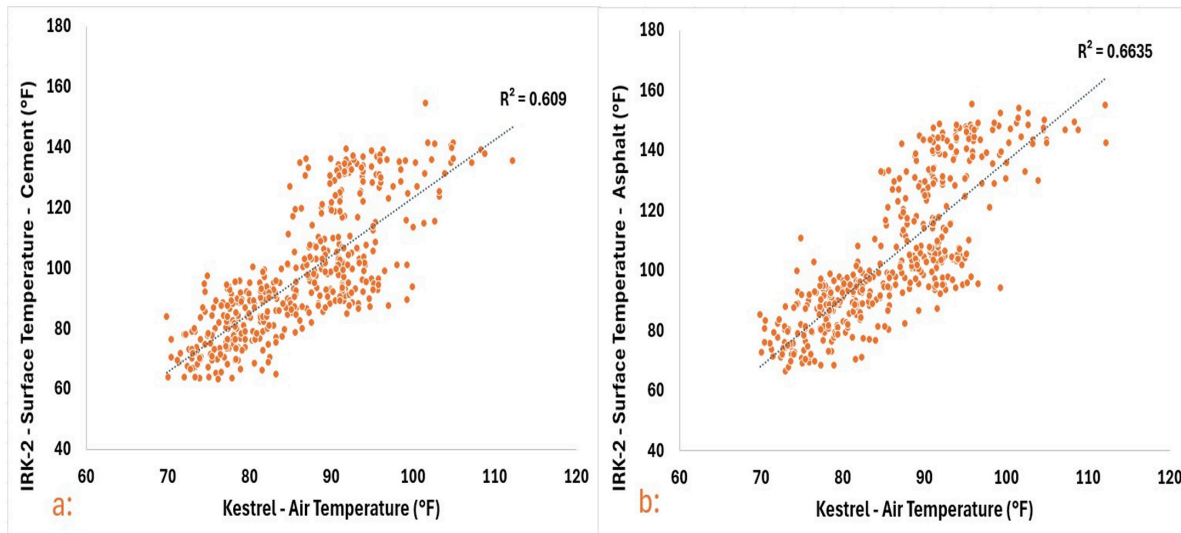


Figure 7. Scatterplot of air temperature versus surface temperature for the different materials encountered during the transect. Left: cement. Right: asphalt.

atmosphere resulting in a decrease in the localized barometric pressure and relative humidity. This effect is comparable to how hot air balloons fly. By heating the air inside the balloon, it makes the air less dense, making the balloon more buoyant, and creating a lift force (ASTROCAMP, 2024).

Heat from the UHI effect drives localized atmospheric convection, which can create its own wind gust fronts. Using the Earth Nullschool visualization tool, we analyzed Convective Available Potential Energy (CAPE) on the dates and times of the observed precipitation events (Figure 8). The data showed significantly higher CAPE during UHI-modified convective precipitation events (133–874 J/Kg) than during natural storm-front precipitation events (9–66 J/Kg) on June 9, 21, and 22. This may suggest a potential correlation between the position of the earth relative to the

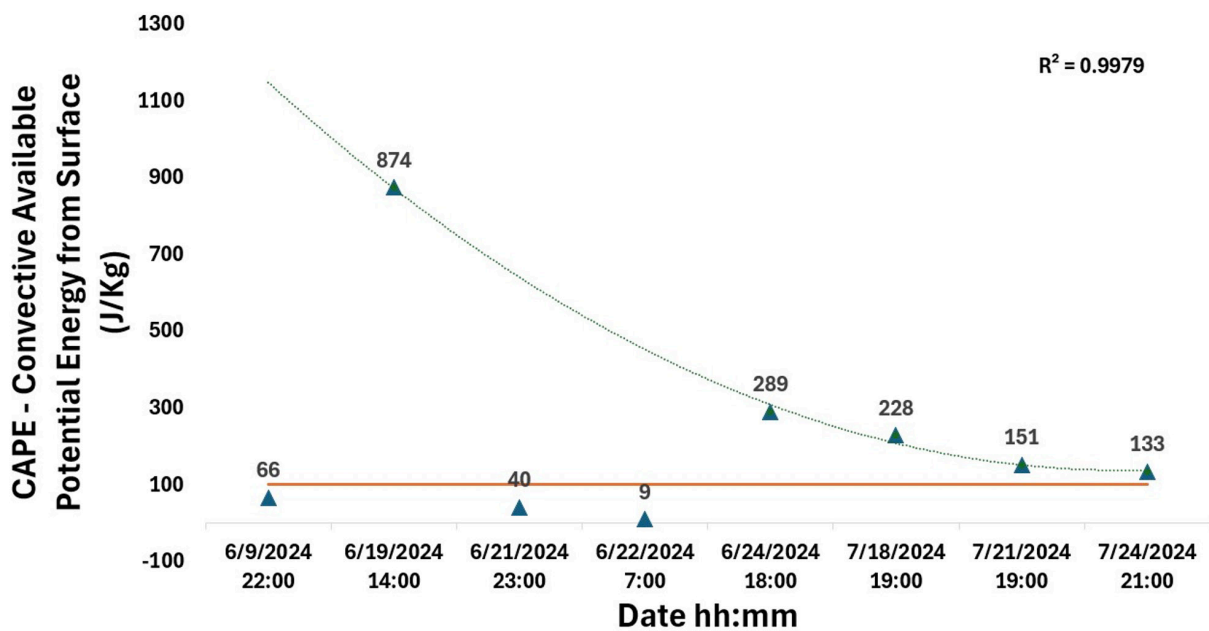


Figure 8. All eight precipitation days recorded during the data collection time, analyzed for CAPE (Convective Available Potential Energy) at the transect site, using Earth Nullschool Modeling tool.

sun and the decreasing intensity of these events after the peak CAPE of 874 J/Kg on June 19, just before the summer solstice on June 20, 2024. Additionally, the  $\Delta T$  temperature spikes seemed to have an inverse relationship with the CAPE data. The  $\Delta T$  temperature spikes increased in intensity as the CAPE declined in intensity.

During UHI precipitation events, water vapor absorbs outgoing infrared radiation from heated urban surfaces. As the heated water vapor rises, it expands and cools, a process known as adiabatic cooling. When this air reaches its dew point, at the condensation level (at approximately 5000 m in Albuquerque), the water vapor condenses around atmospheric suspended fine particles to form a cloud. The latent heat released during this phase change further drives the convection. Thin low clouds may trap outgoing heat and cause a greenhouse effect, they can also reflect incoming short-wave solar radiation, leading to a complex net effect (Figure 9).

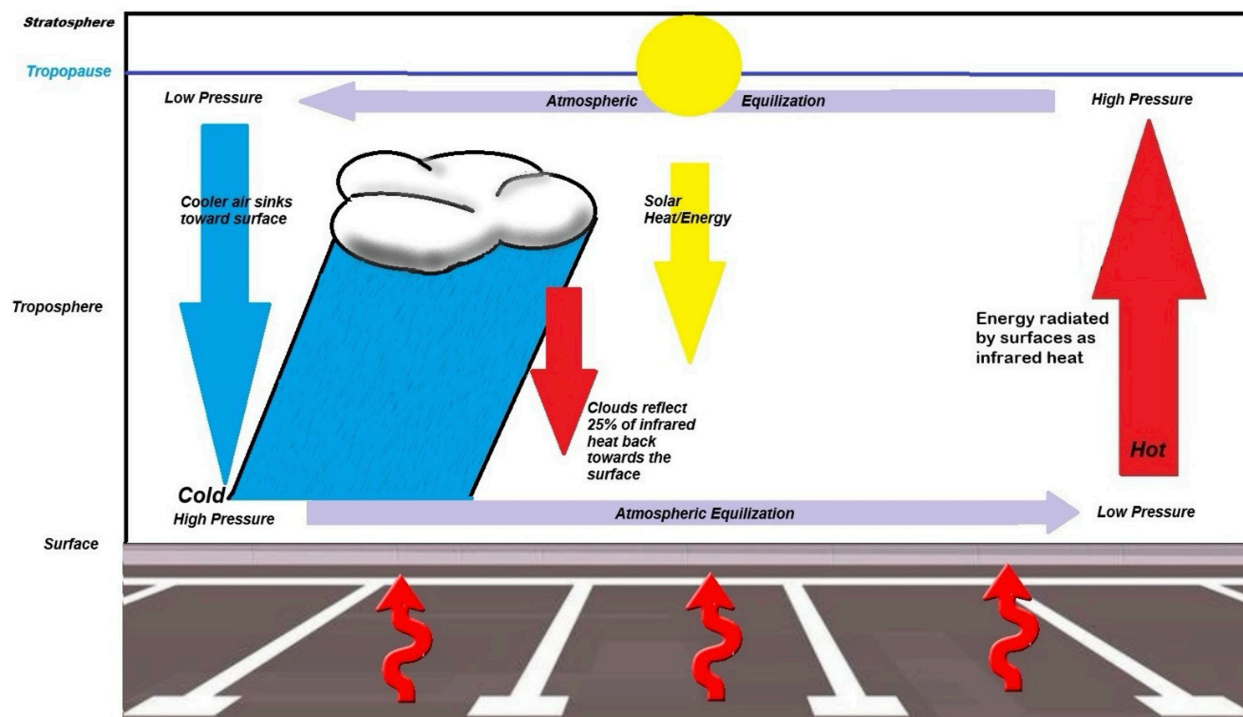


Figure 9. Atmospheric Energy Balance.

Atmospheric convection was observed in our data by wind gusts and drops in barometric pressure, which occur concurrently with the  $\Delta T$  spike and the precipitation events. Additionally, particulates and aerosols in the atmosphere can create an insulating layer that reradiates longwave energy back towards the earth (Toon, 1980). While aerosols may have been a contributor, the data we collected on particulates did not reveal a correlation, the cloud formation above the transect site may have been the leading contributing factor in the initial spike in  $\Delta T$  in the UHI-induced precipitation (Figure 9).

Of note, the UHI-induced precipitation, recorded on July 24, occurred at 9:00 PM, after sunset, when temperatures should have dropped. However, weather station data exhibits a 25 °F  $\Delta T$  spike at the time. (Two of the other UHI-induced precipitation, on June 16 and July 21, had  $\Delta T$  readings of over 30 °F.) This is due to the slower radiation of longwave energy from the asphalt. The asphalt

was still radiating infrared radiation after it ceased receiving solar radiation, causing a UHI-induced precipitation at night.

In this investigation, we found meaningful evidence that a UHI effect is occurring in Albuquerque and is modifying precipitation on a localized level. The magnitude of the  $\Delta T$  was approximately 10 °F higher than expected for this type of UHI but was likely due to the substantial volume of asphalt/concrete surface areas and human/vehicle traffic around the site. Four instances of UHI-induced precipitation were identified during our 8 week study. These instances had  $\Delta T$  spikes preceding precipitation that were well above the 10 °F baseline, and the precipitation originated from clouds that formed over the city of Albuquerque.

Additionally, we found significant evidence that UHI is influencing weather patterns in Albuquerque. The UHI-induced precipitation has a consistent pattern between the five identified days is as follows: high relative humidity and surface temperature earlier in the day, followed by a dramatic drop in relative humidity, surface temperatures, and barometric pressure. Then preceding the precipitation, a spike in  $\Delta T$ .

Future work on this project should include an educational program to inform the public and urban developers about methods to mitigate these UHI effects, to reduce effects on human health and wellbeing (Pine, Aves, Funk, Ahmed, & Kocis, 2023). Additional studies would be necessary to calculate how large a green space is necessary to mitigate the effects of a large asphalt surface area, such as our transect site. While our transect area had a significant number of trees that were planted to mitigate the UHI effect, this effort appears to be insufficient to offset the size and scope of the asphalt surfaces. Larger green spaces would be advised to mitigate the effects in the future.

## **ACKNOWLEDGEMENTS**

This work was funded by NSF grant award 2246468.

## **AUTHOR INFORMATION**

### **Corresponding Author\***

Melanie Will-Cole  
School of Math, Science and Engineering  
Central New Mexico Community College  
Albuquerque, NM 87106  
[mwillcole@cnm.edu](mailto:mwillcole@cnm.edu)

### **Student Researcher**

Heather Fox-Gardner  
Central New Mexico Community College  
Albuquerque, NM 87106  
[hfoxgardner74@unm.edu](mailto:hfoxgardner74@unm.edu)

## REFERENCES

- ASTROCAMP. *Why Do Hot Air Balloons Float?* <https://astrocamp.org/blog/why-do-hot-air-balloons-float/> (accessed 2024-09-20)
- Beccario, C. *"Earth" Nullschool*. <https://earth.nullschool.net/> (accessed 2025-08-25)
- Brown, M. E.; Arnold, D.L. Land-surface-atmosphere interactions associated with deep convection in Illinois. *International Journal of Climatology* **1998**, *18* (15), 1637–1653.
- CAPA Strategies, LLC. *Albuquerque, New Mexico Heat Watch Report*; City of Albuquerque, 2021. [https://www.cabq.gov/sustainability/documents/heat-watch-albuquerque\\_report\\_111921.pdf](https://www.cabq.gov/sustainability/documents/heat-watch-albuquerque_report_111921.pdf)
- Census.gov. *QuickFacts Albuquerque city, New Mexico 2020 April 1*. (accessed from Census.gov 2025 November 20): <https://www.census.gov/quickfacts/fact/table/albuquerquecitynewmexico/POP010220>
- Changnon, J. S. METROMEX: An investigation of inadvertent weather modification. *Bulletin of the American Meteorological Society* **1971**. *52* (10), 958–968.
- Changnon, S. A. The La Porte weather anomaly—fact or fiction? *Bulletin of the American Meteorological Society* **1968**. *49* (1), 4–11. DOI:10.1175/1520-0477-49.1.4
- DATA USA. Tijeras, NM Census Place **2023**. DATA USA (accessed 2025-11-20). [https://datausa.io/profile/geo/tijeras-nm#:~:text=About,\(Hispanic\)%20\(3.52%25\)](https://datausa.io/profile/geo/tijeras-nm#:~:text=About,(Hispanic)%20(3.52%25))
- Ding, M.; Zheng, X. T.; Li, D.; Sun, T. Background wind speeds outweigh urban heat islands in downwind precipitation enhancement by cities. *Geophysical Research Letters* **2025**, *52*. DOI:10.1029/2024GL114142
- Dixon, P. G.; Mote, T. L. Patterns and causes of Atlanta's urban heat island-initiated precipitation. *Journal of Applied Meteorology* **2003**. *42* (9), 1273–1284.
- Easterbrook, D. J. Chapter 9—Greenhouse gases. *Evidence-Based Climate Science*; Easterbrook, D.J., Ed.; Elsevier, **2016**; pp. 163–173. DOI:10.1016/B978-0-12-804588-6.00009-4
- The Engineering Toolbox. *Emissivity Coefficients of Common Materials*. [https://www.engineeringtoolbox.com/emissivity-coefficients-d\\_447.html](https://www.engineeringtoolbox.com/emissivity-coefficients-d_447.html) (accessed 2024-09-04)
- Ganeshan, M.; Murtugudde, R.; Imhoff, M. L. A multi-city analysis of the UHI-influence on warm season rainfall. *Urban Climate* **2013**. *6*. 1–23. DOI:10.106/j.uclim.2013.09.004
- Google. [Satellite imagery of Albuquerque, NM showing data from **2022** October 11 –**2025** August 3,]. Google Earth (accessed 2025-11-19). <https://earth.google.com>
- Google. [Satellite imagery of Albuquerque, NM showing data from **2023** August 25]. Google Earth (accessed 2025-11-15). <https://earth.google.com>
- Horton, R. E. Thunderstorm-breeding spots. *Monthly Weather Review*. **1921**. *49* (4), 193. DOI:10.1175/1520-0493(1921)49<193a:TS>2.0.CO;2

- Jahnke, T. S. Ultrafast energy transfer between water molecules. *Nature Physics* **2010**. 6 (2), 139–142. DOI:10.1038/nphys1498
- NASA Earth Observatory. The Impact of City Landscapes on Rain. *Urban Rain* <https://earthobservatory.nasa.gov/features/UrbanRain/urbanrain2.php#:~:text=Called%20the%20urban%20heat%20island,that%20soak%20the%20area%20downwind>. (accessed 2025-11-22)
- National Weather Service. WPC's Surface Analysis Archive. *Weather Prediction Center*. [https://www.wpc.ncep.noaa.gov/archives/web\\_pages/sfc/sfc\\_archive.php](https://www.wpc.ncep.noaa.gov/archives/web_pages/sfc/sfc_archive.php) (accessed 2025-11-27)
- The Nature Conservancy New Mexico. *Resilient Cities, Remote Sensing: Seeing the City for the Trees: Mapping Albuquerque's Urban Forest*. [https://www.nmconservation.org/field-notes/2018/11/8/seeing-the-city-for-the-trees-albuquerques-urban-forest#:~:text=The%20National%20Agriculture%20Imagery%20Program%20\(NAIP\)%20captured,compared%20to%2093.29%25%20for%20the%20cleaned%20data](https://www.nmconservation.org/field-notes/2018/11/8/seeing-the-city-for-the-trees-albuquerques-urban-forest#:~:text=The%20National%20Agriculture%20Imagery%20Program%20(NAIP)%20captured,compared%20to%2093.29%25%20for%20the%20cleaned%20data) (accessed 2025-11-22)
- Pine, J.; Aves, K.; Funk, K.; Ahmed, Z.; Kocis, K. Urban heat island effect solutions and funding. *National League of Cities*, February 13, 2023. <https://www.nlc.org/article/2023/02/13/urban-heat-island-effect-solutions-and-funding/> (accessed 2024-10)
- Sundborg, A. Local climatological studies of the temperature conditions in an urban area. *Tellus* **1950**, 2 (3), 222–232.
- ThermoWorks. *Infrared Emissivity Table*. <http://www.thermoworks.com/emissivity-table/> (accessed 2024-06).
- Toon, O. B. Atmospheric aerosols and climate. *American Scientist* **1980**. 68 (3), 268–278.
- University of New Mexico. (accessed June 2024). San Pedro Uptown Weather Station. Albuquerque, NM, USA.
- Will-Cole, Melanie. Length-Scale Matters: Revealing the Nature of a Neighborhood-Scale Intra-Urban Heat Island in Albuquerque, NM. American Meteorology Society, *AMS - 105th AMS Annual Meeting*. Jan. 15, 2025. <https://ams.confex.com/ams/105ANNUAL/meetingapp.cgi/Paper/449537> (accessed 2026-02)